5-4-1998

Stability and Reconstruction for an Inverse Problem for the Heat Equations

Kurt M. Bryan
Rose-Hulman Institute of Technology, bryan@rose-hulman.edu

Lester Caudill
University of Richmond

Stability and Reconstruction for an Inverse Problem for the Heat Equation

Kurt Bryan

MS TR 98-01

May 4, 1998

Department of Mathematics
Rose-Hulman Institute of Technology
Terre Haute, IN 47803

FAX (812) 877-3198 **Phone: (812) 877-8391**

Stability and Reconstruction for an Inverse Problem for the Heat Equation *

Kurt Bryan
Department of Mathematics
Rose-Hulman Institute of Technology
Terre Haute, IN 47803

Lester F. Caudill, Jr.
Department of Mathematics and Computer Science
University of Richmond
Richmond, VA 23173

May 4, 1998

Abstract

We examine the inverse problem of determining the shape of some unknown portion of the boundary of a region Ω from measurements of the Cauchy data for solutions to the heat equation on Ω. By suitably linearizing the inverse problem we obtain uniqueness and continuous dependence results. We propose an algorithm for recovering estimates of the unknown portion of the surface and use the insight gained from a detailed analysis of the inverse problem to regularize the inversion. Several computational examples are presented.

Key words. inverse problems, non-destructive testing, thermal imaging.

AMS(MOS) subject classifications. 35A40, 35J25, 35R30

1 Introduction

Thermal imaging is a technique that can be used for fast, non-contact detection and evaluation of defects in materials. It has been used successfully in a variety of nondestructive testing

*This research was supported in part by the NSF under Grant #DMS-9623279.

applications, including the detection and imaging of defects in aircraft [7]. The technique consists of applying a heat flux to the surface of the sample to be imaged, then monitoring the surface temperature response of the sample. From flux-temperature measurements one tries to estimate the internal properties of the sample, or to determine the condition of some inaccessible portion of the sample boundary.

The resulting inverse problem is extremely ill-posed. The flow of heat through an object is of course a diffusive process, and as a result the reconstructions obtained using this method suffer from "blurring" due to the diffusion. Attempts have been made to understand the nature of the blurring, and counteract it, e.g., [5],[6]. In [2] we examined a quasi-steady state version of the problem and the associated blurring due to the ill-posedness of the problem. Other attempts at estimating interior sample properties from boundary measurements have used least-squares estimation techniques, e.g., [1], [4].

In this paper we make a detailed examination of a common problem in thermal imaging—the determination of the shape of some inaccessible portion of a sample's boundary. Specifically, let Ω be an n dimensional box or "slab", $\Omega = \{x \in \mathbb{R}^n;\ 0 < x_k < b_k\}$. We assume that the "front surface" at $x_n = b_n$ is accessible for measurements. The rest of the surfaces, including the "back surface" $x_n = 0$, is considered to be inaccessible and may, under certain conditions, suffer damage or corrosion and so assume the shape $x_n = S(x_1, \ldots x_{n-1})$. The goal is to determine the function S by making measurements on the accessible portion of the boundary.

In [3] we established that the inverse problem of determining the shape of an inaccessible portion of the boundary of a sample from thermal measurements is uniquely solvable given some modest restrictions on the domain and input heat flux. The results are applicable here—the boundary can, in principle, be determined. In this paper we consider a linearized version of the inverse problem and use this to establish a simple relation between the input flux, back surface profile S, and measured data. In some ways our approach is similar to that of [5], in which the authors linearize by establishing a Born approximation for the front surface data in order the reconstruct the back surface. However, our results hold for any type of back surface or input flux. Although our main interest is stability and reconstruction, we also establish a uniqueness result for reasonable input fluxes. For the most common case in which the input flux is spatially constant (but a function of time) we establish sharp stability estimates for the inversion process and develop an algorithm for estimating the back surface profile from front surface measurements. Finally, we present computational examples. Our analysis and results hold for regions in any dimension $n \geq 2$, but we present computational examples only for two dimensional domains.

The paper is organized as follows. In section 2 we give a careful statement of the forward and inverse problems, and construct a linearized version of the inverse problem, that is, we linearized the relationship between the back surface described by $x_n = S(x_1, \ldots, x_{n-1})$ and the temperature data. In section 3 we establish an integral equation which relates S to the front surface data and use this relation to establish uniqueness for the linearized inverse problem under realistic assumptions on the input flux and initial condition. Finally, in section 4 we use this relation to examine the stability of inversions in the case in which the input flux varies in time, but is spatially constant. We present an algorithm for recovering estimates of the back surface and show a number of examples.

2 The Forward and Inverse Problems

2.1 Notation and Geometry

We will use $x = (x_1, \ldots, x_n)$ to denote a point in $\mathbb{R}^n$ and will write $x = (x', x_n)$ with $x' = (x_1, \ldots, x_{n-1})$ to distinguish the nth component of x. Let B denote a box in $n-1$ dimensions, of the form $x' \in \mathbb{R}^{n-1}$ with $0 < x_k < b_k$ for some b_k, $1 \leq k \leq n-1$. Let Ω_0 denote the n-dimensional box consisting of points $x = (x', x_n)$ with $x' \in B$ and $0 < x_n < d$, where d is a constant which denotes the thickness of Ω_0. The n-dimensional box Ω_0 represents the undamaged or reference configuration of the sample to be tested. The region Ω_0 is bounded, but with minor modification our results also hold for unbounded regions, e.g., in which $B = \mathbb{R}^{n-1}$. We will highlight this at the appropriate point.

Let Ω denote the damaged sample whose boundary is to be determined. We take Ω to consist of points $x = (x', x_n)$ with $x' \in B$, $S(x') < x_n < d$, where S is a C^2 function defined on B with $\text{supp}(S) \subset B$. The value of S represents the amount of material loss in the sample. Of course, material "loss" dictates that $S \geq 0$, although this restriction is not mathematically required. The requirement that S be C^2 will later be relaxed. We use Γ_1 to denote the top surface of the sample, (x', d), with $x' \in B$. Γ_1 is that portion of the boundary of Ω which is accessible for measurements. Let Γ_0 denote the "back" surface of the sample, $(x', S(x'))$ with $x' \in B$.

2.2 The Forward Problem

The function $u(t, x)$ will be used to denote the temperature of the sample at position x and time t. The forward problem which models the flow of heat through the sample Ω (or Ω_0) is

$$\begin{aligned} \frac{\partial u}{\partial t} - \alpha \triangle u &= 0 \text{ in } (0, \infty) \times \Omega, \\ \kappa \frac{\partial u}{\partial \nu} &= g(t, x') \text{ on } \Gamma_1, \\ \kappa \frac{\partial u}{\partial \nu} &= 0, \text{on } \partial\Omega \setminus \Gamma_1, \\ u(0, x) &= f(x). \end{aligned} \tag{2.1}$$

Here $\alpha > 0$ is the thermal diffusivity of the sample (assumed constant, and with temperature variation sufficiently small that α is independent of u). The constant $\kappa > 0$ is the thermal conductivity of the sample (with the same assumptions as α), and $g(t, x')$ is the input heat flux applied to the top surface at time t at the point (x', d). We will assume that g has compact support in time and is not identically zero. The vector ν is the outward unit normal on $\partial\Omega$. Note that we are modeling the unknown portion of the boundary of Ω as a perfect thermal insulator.

We have included the physically relevant constants κ, α, and d, since the conditioning of the inverse problem depends heavily on the relative values of these parameters and is therefore of practical interest. However, for now we introduce rescaled dimensionless variables $\tilde{x} = x/d$ and $\tilde{t} = \frac{\alpha}{d^2} t$ and define $\tilde{u}(\tilde{t}, \tilde{x}) = \frac{\kappa}{d} u(t, x) = \frac{\kappa}{d} u(\frac{d^2}{\alpha} \tilde{t}, d\tilde{x})$. The heat equation (2.1) then becomes,

$$\frac{\partial \tilde{u}}{\partial \tilde{t}} - \Delta \tilde{u} = 0 \text{ in } (0, \infty) \times \tilde{\Omega}, \tag{2.2}$$

$$\frac{\partial \tilde{u}}{\partial \nu} = \tilde{g}(\tilde{t}, \tilde{x}), \text{ on } \tilde{\Gamma}_1, \tag{2.3}$$

$$\frac{\partial \tilde{u}}{\partial \nu} = 0, \text{ on } \tilde{\Gamma}_0, \tag{2.4}$$

$$\tilde{u}(0,\tilde{x}) = \tilde{f}(\tilde{x}). \tag{2.5}$$

with $\tilde{g}(\tilde{t},\tilde{x}) = g(\frac{d^2}{\alpha}\tilde{t}, d\tilde{x}')$ and $\tilde{f}(\tilde{x}) = \frac{\kappa}{d}f(d\tilde{x})$. Here $\tilde{\Gamma}_0$ denotes the rescaled back surface $(\tilde{x}', \tilde{S}(\tilde{x}'))$ with $\tilde{S}(\tilde{x}') = \frac{1}{d}S(d\tilde{x}')$ and $\tilde{\Gamma}_1$ denotes the surface $(x', 1)$. $\tilde{\Omega}$ is the region bounded by $\tilde{\Gamma}_0$ and $\tilde{\Gamma}_1$ on top and bottom, and dB on the "sides".

We will continue our analysis with the rescaled problem (2.2)-(2.5), but will omit the tilde's on the variables and domains.

2.3 The Inverse Problem

The inverse problem is this:

Let $u(t,x)$ satisfy the initial-boundary value problem (2.2)-(2.5) with known input flux $g(t,x')$. We may or may not consider the initial temperature $f(x)$ as known. Given measurements of $u(t,x)$ for $x \in \Gamma_1$ over a time interval (t_1,t_2), determine the back surface $x_n = S(x')$.

The relevant questions are:

- Under what conditions is the back surface uniquely determined?
- How stable is any inversion with respect to noise in the temperature and flux measurements?
- How can one efficiently recover an estimate of the back surface?

In [3] we proved that for any bounded region (not necessarily of the form described above), knowledge of the flux-temperature data on any open portion of $\partial\Omega$ and over a "sufficiently large" time interval uniquely determines the unknown portion of the boundary (in this case, $(x', S(x'))$) and the initial condition, provided the input flux satisfies certain assumptions. If one know a priori that the initial data f is constant, then knowledge of the flux-temperature data over *any* time interval suffices to determine the unknown portion of the boundary.

However, with no assumptions on the input flux and initial condition one can construct counterexamples to uniqueness.

The main focus of this paper is the latter two questions posed above, although along the way we prove some uniqueness results.

2.4 The Linearized Inverse Problem

In this section we derive an approximate linearized relationship between S and u. We begin with a change of coordinates. Let $\phi : \mathbb{R}^n \to \mathbb{R}^n$ denote the map

$$(x', x_n) \to \left(x', \frac{x_n - S(x')}{1 - S(x')}\right)$$

for $x' \in B$, $S(x') < x_n < 1$. Then ϕ maps the sample region Ω into the region Ω_0 while keeping $\Gamma_1 fixed.$ Also, since $S(x') < 1$, it's easy to see that ϕ is invertible. Define the function $v(t,x) = u(t, \phi^{-1}(x))$ on Ω_0, where $u(t,x)$ satisfies (2.2)-(2.5). It is not difficult to check that $v(t,x)$ satisfies the equation

$$\frac{1}{|D\phi|}\frac{\partial v}{\partial t} - \nabla \cdot \gamma \nabla v = 0 \tag{2.6}$$

in $(0,\infty) \times \Omega_0$, where $D\phi$ denote the Jacobian of ϕ, $|D\phi|$ the determinant, and $\gamma = (D\phi)(D\phi)^T/|D\phi|$. The boundary and initial conditions (2.3)-(2.5) become

$$\frac{\partial v}{\partial \eta} = g(t,x') \text{ on } R_1, \tag{2.7}$$

$$\frac{\partial v}{\partial \eta} = 0 \text{ on } \partial\Omega_0 \setminus R_1, \tag{2.8}$$

$$v(0,x) = f(\phi^{-1}(x)) \tag{2.9}$$

where $\eta = (D\phi)\nu$. Here R_1 denotes the top surface of Ω_0, $\{(x',1); x' \in B\}$. We will use R_0 to denote the bottom surface $\{(x',0); x' \in B\}$.

Let us now formally linearize the forward problem about $S = 0$. Let $u_0(t,x)$ denote the solution to (2.2)-(2.5) with $S \equiv 0$ (so $u_0(t,x)$ is defined for $x \in \Omega_0$). Let us assume that $S(x')$ is "small" and that $v(t,x) = u_0(t,x) + w(t,x)$ with w also small. Note that w is the perturbation in the temperature response due to the material loss in the sample. If we put

$v = u_0 + w$ into equations (2.6)-(2.9), expand, drop quadratic terms, and use the fact that u_0 satisfies (2.2)-(2.5) on $(0, \infty) \times \Omega_0$, we find that to first order $w(t,x)$ satisfies

$$
\begin{aligned}
\frac{\partial w}{\partial t} - \Delta w &= \nabla \cdot \gamma \nabla u_0 + S(x') \Delta u_0 \text{ in } (0,\infty) \times \Omega_0, && (2.10)\\
\frac{\partial w}{\partial \nu} &= -S(x') g(t,x') \text{ on } R_1, && (2.11)\\
\frac{\partial w}{\partial \nu} &= -\nabla S \cdot \nabla u_0, \text{on } \partial\Omega_0 \setminus R_1, && (2.12)\\
w(0,x) &= (1-x_n) \frac{\partial f(x)}{\partial x_n} S(x') && (2.13)
\end{aligned}
$$

where ∇S denotes the gradient of S thought of as a function of n variables which happens to be independent of x_n. The matrix γ can be written out explicitly as

$$\gamma(x', x_n) = \begin{pmatrix} -S(x') I_{n-1} & (x_n - 1)\nabla' S \\ (x_n - 1)(\nabla' S)^T & S(x') \end{pmatrix}$$

where I_{n-1} is the $n-1$ by $n-1$ identity matrix and the column vector $\nabla' S$ is the gradient of S as a function of variables $x_1, \ldots, x_{n-1}$. Equations (2.10)-(2.13) define a linear relation between S and w.

It is this linearized version of the heat conduction inverse problem that we will analyze.

3 Integral Representation of the Solution

Define $d(t,x') = w(t,x',1)$ where w satisfies (2.10)-(2.13). The function $d(t,x')$ is the temperature data from the accessible portion of $\partial\Omega$. Given the linear relation between S and w (and hence d), the function $d(t,x')$ can be expressed as an appropriate weighted integral of $S(x')$. This is the focus of the following Lemma 3.1 below. In what follows we use $\nabla'\phi$ to denote the gradient of a function ϕ in variables $x_1, \ldots, x_{n-1}$ and $\Delta'\phi$ to denote the Laplacian of ϕ in the first $n-1$ variables.

Lemma 3.1 *Let $\phi(t,x)$ be a solution to the heat equation $\frac{\partial \phi}{\partial t} - \Delta\phi = 0$ on $(0,T) \times \Omega_0$ with $\frac{\partial \phi}{\partial \nu} \equiv 0$ on $\partial\Omega_0 \setminus R_1$ and $\phi(0,x) = 0$ for $x \in \Omega_0$. Then*

$$
\begin{aligned}
&\int_0^T \int_{R_1} d(t,x') \frac{\partial \phi}{\partial \nu}(T-t,x',1)\, dx'\, dt && (3.14)\\
= &\int_0^T \int_{R_0} S(x') [\nabla' \phi(T-t,x',0) \cdot \nabla' u_0(t,x',0) + \phi(T-t,x',0) \Delta' u_0(t,x',0)]\, dx'\, dt.
\end{aligned}
$$

Note that by standard regularity results for the heat equation the functions u_0 and ϕ are smooth on R_0—indeed, they are analytic and extend as analytic solutions of the heat equation across R_0. Thus the quantity multiplying $S(x')$ under the integral on the right in Lemma 3.1 is well-defined.

The proof of Lemma 3.1 amounts to nothing more than a rather tedious calculation involving repeated use of Green's identities, integration by parts, equations (2.10)-(2.13), and the equations satisfied by ϕ and u_0. We relegate it to an appendix.

3.1 Good Test Functions and Uniqueness

We now construct a class of test functions $\phi(t,x)$ to be used in the integral representation (3.14). These functions allow us to extract specific information about the function S from the front surface data d. Let $\lambda = (\lambda_1,\ldots,\lambda_{n-1})$ denote an $n-1$ dimensional real-valued vector with $\lambda_k = j\pi/b_k$, j and integers; we will write λ^2 to denote $\lambda\cdot\lambda$. Define

$$c(\lambda,x') = \cos(\lambda_1 x_1)\cos(\lambda_2 x_2)\cdots\cos(\lambda_{n-1}x_{n-1}).$$

Then for a function $\phi(x')$ defined on B the integral $\int_B c(\lambda,x')\phi(x')\,dx'$ is a coefficient in the (multiple) Fourier cosine expansion of ϕ over B. In particular, as λ ranges over all permissible values the set $c(\lambda,x')$ forms an orthogonal basis for $L^2(B)$. Let us use the notation $\hat{f}(s,x)$ for the Laplace transform of a function $f(t,x)$ with respect to t.

Lemma 3.2 *For $c(\lambda,x')$ as defined above we have*

$$\begin{aligned} &\int_B c(\lambda,x')\hat{d}(s,x')\,dx' \qquad (3.15)\\ &= \frac{1}{\sqrt{s+\lambda^2}\sinh(\sqrt{s+\lambda^2})}\int_B c(\lambda,x')\left[-\nabla' S(s,x')\cdot\nabla' u_0(s,x',0) + S(x')\frac{\partial^2 u_0}{\partial x_n^2}(s,x',0)\right]dx'. \end{aligned}$$

Proof: Let $\phi_0(t,x_n)$ denote the unique solution to

$$\begin{aligned} \frac{\partial\phi_0}{\partial t} - \frac{\partial^2\phi_0}{\partial x_n^2} &= -\lambda^2\phi_0, \quad 0 < \mathrm{x_n} < 1 \qquad (3.16)\\ \frac{\partial\phi_0}{\partial x_n}(t,1) &= h(t),\\ \frac{\partial\phi_0}{\partial x_n}(t,0) &= 0,\\ \phi_0(0,x_n) &= 0. \end{aligned}$$

Here $h(t)$ is any sufficiently smooth input heat flux. That ϕ_0 is unique is easy to show. (We will in fact explicitly construct ϕ_0 later.) Define $\phi(t,x) = \phi_0(t,x_n)c(\lambda,x')$. The function $\phi(t,x)$ satisfies the heat equation on $\Omega_0 = B \times (0,1)$. Also, $\phi(0,x) \equiv 0$. We have that $\frac{\partial \phi}{\partial \nu} \equiv 0$ on the bottom surface R_0. With λ_k chosen as $\lambda_k = j\pi/b_k$ where j is any integer, we have $\frac{\partial \phi}{\partial \nu} \equiv 0$ on the "sides" of Ω_0, so that $\frac{\partial \phi}{\partial \nu} \equiv 0$ on $\partial\Omega_0 \setminus R_1$. The function ϕ is then a legitimate test function for (3.14), which now takes the form

$$\int_B c(\lambda,x') \left(\int_0^T d(t,x')h(T-t)\,dt \right) dx'\,dt = \tag{3.17}$$
$$\int_B S(x') \left(\int_0^T \phi_0(T-t,0)[\nabla' c(\lambda,x') \cdot \nabla' u_0(t,x',0) + c(\lambda,x') \triangle u_0(t,x',0)]\,dt \right) dx'\,dt,$$

where we have used $\nabla\phi = (\phi_0 \nabla c, 0)$ on R_0, and noted that the integration is really over the box B. Given the assumptions on Ω_0, S, and the smoothness of the functions involved, the interchange of integration is certainly permissible.

Now Laplace transform both side of equation (3.17) with respect to T. Using the elementary convolutional properties of the Laplace transform (again, with justifiable interchange of integrals) we obtain

$$\begin{aligned} & \hat{h}(s) \int_B c(\lambda,x')\hat{d}(s,x')\,dx' \\ = \; & \hat{\phi}_0(s,0) \int_B S(x')\,[\nabla' c(\lambda,x') \cdot \nabla' \hat{u}_0(s,x',0) + c(\lambda,x') \triangle \hat{u}_0(s,x',0)]\,dx', \end{aligned} \tag{3.18}$$

where $\hat{h}(s)$ denotes the Laplace transform of h, etc. We can in fact write out $\hat{\phi}_0(s,0)$ by Laplace transforming the one-dimensional heat equation (3.16) and solving the resulting two-point boundary value problem, to find that $\hat{\phi}_0(s,0) = 2\hat{h}(s)/(\sqrt{s+\lambda^2}\sinh(\sqrt{s+\lambda^2}))$. Substituting this into equation (3.18) shows that

$$\begin{aligned} & \int_B c(\lambda,x')\hat{d}(s,x')\,dx' \\ = \; & \frac{1}{\sqrt{s+\lambda^2}\sinh(\sqrt{s+\lambda^2})} \int_B S(x')\,[\nabla' c(\lambda,x') \cdot \nabla' \hat{u}_0(s,x',0) + c(\lambda,x') \triangle \hat{u}_0(s,x',0)]\,dx'. \end{aligned} \tag{3.19}$$

Note that $\hat{h}$ cancels—the temporal behavior of the test function is irrelevant.

If we integrate the first term under the integral on the right by parts, and use the fact that S is supported in a compact subset of B we obtain exactly Lemma 3.2.■

3.2 Uniqueness for the Linearized Inverse Problem

We can use Lemma 3.2 to prove that the data d determines the back surface S under a variety of conditions on the input flux g. We consider three cases:

Lemma 3.3 *Let the input flux satisfy one of the conditions*

1. *The input flux is independent of x', so $g = g(t)$.*
2. *The input flux is nonnegative, $g(t, x') \geq 0$.*
3. *The input flux is of the form $g(t, x') = \cos(\frac{\pi}{b_j} x_j)$, $1 \leq j \leq n-1$.*

with the solution w to the linearized problem (2.10)-(2.13) with constant initial condition. In all cases we of course assume that the flux is not identically zero. Then the data $d(t, x') = w(t, x', 1)$ for $t > 0$ determines the function $S(x')$.

Proof: In any case to prove uniqueness it suffices by linearity to show that if $d \equiv 0$ then $S \equiv 0$. Hence let us assume that $d \equiv 0$ for $t > 0$ and so $\hat{d} \equiv 0$. In this case, since $\frac{1}{\sqrt{s+\lambda^2}\sinh(\sqrt{s+\lambda^2})} \neq 0$ we conclude that the integral on the right in Lemma 3.2 vanishes for all λ. Since $c(\lambda, x')$ forms a complete orthonormal set as λ ranges over all appropriate values, we conclude that $-\nabla' S(x') \cdot \nabla' \hat{u}_0(s, x', 0) + S(x') \frac{\partial^2 \hat{u}_0}{\partial x_n^2}(s, x', 0) = 0$ for $x' \in B$ and all $s > 0$. Inverse Laplace transforming shows that

$$- \nabla' S(x') \cdot \nabla' u_0(t, x', 0) + S(x') \frac{\partial^2 u_0}{\partial x_n^2}(t, x', 0) = 0 \tag{3.20}$$

in B, for all $t > 0$.

To prove case (1) in the Lemma, we note that if $g = g(t)$ is independent of x' then so is $u_0(t, x', x_n)$ satisfying (2.2)-(2.5) (with $S \equiv 0$ and zero initial condition). In this case equation (3.20) becomes $S(x') \frac{\partial^2 u_0}{\partial x_n^2}(t, x', 0) = 0$ for $x' \in B$ and $t > 0$. As noted earlier, the function $u_0(t, x)$ is analytic near R_0. We can conclude that the function $u_1(t, x) = \frac{\partial u_0}{\partial x_n}$ is itself a solution to the heat equation near R_0 and, since $\frac{\partial u_0}{\partial x_n} = 0$ on R_0, we have $u_1(t, x', 0) \equiv 0$ on R_0. But if $S \neq 0$ then $S \frac{\partial^2 u_0}{\partial x_n^2} = 0$ forces $\frac{\partial u_1}{\partial x_n} = 0$ on some open neighborhood in B. Since u_1 has zero Cauchy data on an open subset of B over an open time interval, we conclude that $u_1 \equiv 0$. This forces u_0 to be a constant, contradicting $g \neq 0$. This proves case (1).

To prove case (2), we use the identity $\nabla' u_0 \cdot \nabla' S = \nabla' \cdot (S \nabla' u_0) - S \triangle' u_0$ in conjunction with equation (3.20) to obtain

$$-\nabla' \cdot (S \nabla' u_0) + S \triangle u_0 = 0$$

in B, for all $t > 0$. If we integrate this over B and apply the divergence theorem, noting that S has compact support, we obtain $\int_{R_0} S \triangle u_0 \, dx' = 0$ or, since u_0 satisfies the heat equation

$$\int_{R_0} S \frac{\partial u_0}{\partial t} \, dx' = 0.$$

We can conclude that $\frac{\partial}{\partial t} \int_{R_0} S u_0 \, dx' = 0$, so $\int_{R_0} S u_0 \, dx'$ is constant in time. However, a simple argument using the maximum principle and the fact that $g(t,x) > 0$ shows that $\frac{\partial u_0}{\partial t}(t, x', 0) > 0$ a.e. on R_0. If $S > 0$ on any open interval we conclude that $\int_{R_0} S u_0 \, dx'$ cannot be constant. The establishes uniqueness in case (2).

To prove case (3), we note that equation (3.20) defines, for each t, a first order linear PDE for the function $S(x')$. If $g(t, x') = \cos(\lambda_j x_j)$ then the function $u_0(t,x)$ is of the form $h(t, x_n) \cos(\frac{\pi}{b_j} x_j)$ (with zero initial conditions). At any time $t > 0$ the vector field $\nabla' u_0(t, x', 0)$ is of the form $-\frac{\pi}{b_j} \sin(\frac{\pi}{b_j} x_j) \mathbf{e}_j$ where $\mathbf{e}_j$ is the $n-1$ dimensional unit vector in the x_j direction. It's easy to see that $\nabla' u_0$ is noncharacteristic for any surface of the form $x_j = b$ with b constant and that since S is compactly supported in B we have $S \equiv 0$ on $x_j = b$ for some b with $0 < b < b_j$. On such a surface S has zero "initial data" and integrating equation (3.20) along the characteristics of $\nabla' u_0$ across B shows that $S \equiv 0$ in B.■

Remark 3.1 *It is not clear what the weakest conditions are which can be imposed on the input flux and/or initial conditions to obtain uniqueness for the linearized inverse problem. However, uniqueness does NOT hold without some additional conditions on S, g, and/or the initial condition. For example, consider $\Omega_0 = (0,1)^2$ in two dimensions and let $u_0(t, x_1, x_2) = e^{-(b^2+9\pi^2)t} \cos(3\pi x_1) \cos(b x_2)$ where b is any constant. This function satisfies the heat equation in Ω_0 with $\frac{\partial u_0}{\partial \nu} = 0$ on the bottom and sides of Ω_0, and nonzero flux on top (if b is not a multiple of π). However, equation (3.20) is satisfied for all $t > 0$ by any multiple of the function*

$$S(x_1) = \begin{cases} 0, & 0 < x_1 \le \frac{1}{3}, \\ (-\sin(3\pi x_1))^{\frac{b^2}{9\pi^2}}, & \frac{1}{3} < x_1 < \frac{2}{3}, \\ 0, & \frac{2}{3} \le x_1 < 1. \end{cases}$$

If we choose $b > 3\pi$ then S is C^1. Thus a nonzero S yields zero boundary data in the linearized problem for an appropriate combination of input flux and initial data. This counterexample is similar to those we presented in [3] for the full nonlinear inverse problem. Analogous counterexamples can be produced in higher dimensions.

However, in the general case it is not hard to see that if S is NOT uniquely determined, so that equation (3.20) holds, then the vector field $\nabla' u_0$ must be characteristic for the boundary of $\text{supp}(S)$ (wherever $\partial(\text{supp}(S))$ is suitably smooth), i.e., $\frac{\partial u_0}{\partial \nu} \equiv 0$ on $\partial(\text{supp}(S))$. If $\nabla' u_0$ were noncharacteristic on some portion of $\partial(\text{supp}(S))$ then one could use equation (3.20) to show that $S \equiv 0$ inside some region of $\text{supp}(S)$, a contradiction.

Remark 3.2 *It is interesting that under the most natural physical conditions—$S \geq 0$ and $g \geq 0$—one obtains a uniqueness result.*

Remark 3.3 *In the case that $B = \mathbb{R}^{n-1}$ (so the sample is unbounded) one can still linearize and construct an integral representation analogous to Lemma 3.1, if S has compact support. If we consider test functions of the form*

$$c(\lambda, x') = e^{i(\lambda \cdot x')}$$

where $\lambda \in \mathbb{R}^{n-1}$ then we find that Lemma 3.2 also holds. The left side of equation (3.15) becomes the Fourier transform with respect to the spatial variables of $\hat{d}(s, x')$.

The uniqueness proof in cases (1) and (2) also carries through, although there is no obvious analogy for the third case.

4 Stability and Reconstruction for Spatially Constant Flux

In this section we make a more detailed examination of the structure of the inverse problem for the most physically relevant flux in which $g = g(t)$ is a function only of time. This is typically the case when the flux is provided by heat or flash lamps applied to the surface of the sample.

4.1 Spatially Constant Input Flux

We will assume that the input flux is of the form $g = g(t)$. If $u_0(t,x)$ satisfies (2.2)-(2.5) with $S \equiv 0$ and zero initial condition then u_0 is a function only of t and x_n. One can Laplace transform the resulting one-dimensional heat equation to find that

$$\hat{u}_0(s, x_n) = \frac{\hat{g}(s)\cosh(x_n\sqrt{s})}{\sqrt{s}\sinh(\sqrt{s})}. \tag{4.21}$$

It is then simple to see that $\frac{\partial^2 \hat{u}_0}{\partial x_n^2} = s\hat{u}_0(s, x_n)$. Substituting this into equation (3.15) produces

$$\hat{d}(s, \lambda) = M(s, \lambda)\hat{g}(s)\hat{S}(\lambda) \tag{4.22}$$

where $\hat{d}(s, \lambda, x')$ is the Laplace transform in t of the Fourier cosine coefficient corresponding to λ, $\hat{g}(s)$ is the Laplace transform of $g(t)$, and $\hat{S}(\lambda)$ is the Fourier cosine coefficient of S at frequency λ. The function $M(s, \lambda)$ is given by

$$M(s, \lambda) = \frac{\sqrt{s}}{\sqrt{s+\lambda^2}\sinh(\sqrt{s+\lambda^2})\sinh(\sqrt{s})}. \tag{4.23}$$

One could attempt to reconstruct $S(x')$ using equation (4.22) as follows: First, compute $\hat{d}(s, \lambda, x')$ by computing $\int_B d(t, x')c(\lambda, x')\,dx'$, the Fourier coefficient of $d(t, x')$, and then Laplace transform in t (or vice-versa—transform and then compute the coefficient. Given the smoothness assumptions it won't matter). Then divide by $M(s, \lambda)\hat{g}(s)$; according to equation (4.22), this gives $\hat{S}(\lambda)$. One can then compute $S(x')$ from its Fourier cosine expansion. However, it is clear from equation (4.22) that the inversion process will be extremely ill-posed, with spatial frequencies λ in the data weighted essentially by $|\lambda|e^{|\lambda|}$ in the inverted Fourier transform. This is similar to the result we obtained in [2] for the quasi-steady state version of the problem.

We note also that if $g(t) \geq 0$ then for any fixed "frequency" $s > 0$ such a reconstruction is always possible, for $M(s, \lambda) > 0$ and $g(t) \geq 0$ implies $\hat{h}(s) > 0$ for all $s > 0$, and so we never divide by zero. In this case the measured data at any fixed s always encodes the information needed to determine $\hat{S}(\lambda)$.

Actually, we can inverse Laplace transform equation (4.22) explicitly and provide additional insight into the relationship between S and d, especially the time dependence of that data d. We assume that $g(t)$ is supported in an interval $[0, T]$, and that we wish to compute the inverse transform at a time $t > T$ (after the input flux has been turned off).

Lemma 4.1 *Let $g(t)$ be supported in an interval $t \in [0,T]$. Then for $t > T$ the inverse Laplace transform of $M(s,\lambda)\hat{g}(s)$ is given by*

$$K(t,\lambda) = r_2(0)e^{-\lambda^2 t} + \sum_{j=1}^{\infty} \left[r_1(j)\hat{g}(-j^2\pi^2)e^{-j^2\pi^2 t} + r_2(j)\hat{g}(-j^2\pi^2 - \lambda^2)e^{-(j^2\pi^2+\lambda^2)t} \right] \quad (4.24)$$

where

$$r_1(j) = \frac{2(-1)^{j+1}j^2\pi^2}{\sqrt{\lambda^2 - j^2\pi^2}\sinh(\sqrt{\lambda^2 - j^2\pi^2})}, \quad (4.25)$$

$$r_2(j) = \frac{2(-1)^j\sqrt{\lambda^2 + j^2\pi^2}}{\sin(\sqrt{\lambda^2 + j^2\pi^2})}, \quad (4.26)$$

for $j \geq 1$, and $r_2(0) = \frac{\lambda\hat{g}(-\lambda^2)}{\sin(\lambda)}$.

Proof: If the flux $g(t)$ is supported in an interval $t \in [0,T]$ then $\hat{g}(s)$ (considered as a complex-valued function) is analytic in the complex plane. It is not difficult to check that despite the square roots and whatever branch is chosen for them, the function $M(s,\lambda)$ as a function of s is in fact analytic in the complex plane, except for isolated poles along the negative real axis. We can inverse Laplace transform $M(s,\lambda)\hat{g}(s)$ (which we denote by $K(t,\lambda)$) as

$$K(t,\lambda) = \frac{1}{2\pi i}\int_{a-i\infty}^{a+i\infty} e^{st}M(s,\lambda)\hat{g}(s)\,ds. \quad (4.27)$$

(see, e.g., [8], Volume 2) where the integration is along the strip $a + ui$, $u = -\infty$ to $u = \infty$ with $a > 0$. Simple estimates show that the integral converges for $t > T$.

Given that the integral converges and that $e^{st}M(s,\lambda)\hat{g}(s)$ is analytic except at poles on the negative real axis, we may attempt to evaluate $K(t,\lambda)$ with a contour integral. The details of the inversion depend slightly on the value of λ^2, but in the case in which $\lambda^2 \neq \pi^2(k^2 - j^2)$ for integers j,k, we find that M has simple poles at $s = -k^2\pi^2$ and at $s = -k^2\pi^2 - \lambda^2$ for $k \in \mathbf{Z}$, $k \geq 1$. If $\lambda^2 \neq 0$ then the singularity at $s = 0$ is removable. Consider a contour in the complex plane as in Figure 1. It is straightforward to estimate that the integral of $M(s,\lambda)\hat{g}(s)$ over the pieces $s = u + bi$ and $s = u + di$ approaches zero as $b, d \to \infty$.

For the integral over $s = c + iu$, if we assume that $t > T$ (so we are attempting to evaluate $K(t,\lambda)$ after the input flux has been turned off) we can also show that the integral of $M(s,\lambda)\hat{g}(s)$ over $s = c + iu$ approaches zero as $c \to -\infty$, provided we choose c so that the path does not pass through the poles of M. Specifically, since $g(t)$ is supported in $[0,T]$

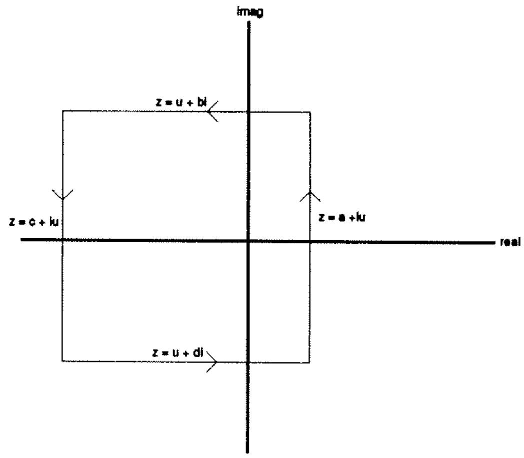

Figure 1

we have $|\hat{g}(s)| \leq Ce^{-sT}$, and using $s = c + iu$ with u real we obtain

$$
\begin{aligned}
& \left| \int_{c-i\infty}^{c+i\infty} e^{st} \frac{e^{st}\hat{g}(s)\sqrt{s}\,ds}{\sinh(\sqrt{s})\sinh(\sqrt{s+\lambda^2})\sqrt{s+\lambda^2}} \right| \\
\leq\; & C \left| \int_{c-i\infty}^{c+i\infty} \frac{e^{s(t-T)}\sqrt{s}\,ds}{\sinh(\sqrt{s})\sinh(\sqrt{s+\lambda^2})\sqrt{s+\lambda^2}} \right| \\
\leq\; & Ce^{c(t-T)} \left| \int_{-\infty}^{\infty} \frac{\sqrt{c+iu}\,du}{\sinh(\sqrt{c+iu})\sinh(\sqrt{c+iu+\lambda^2})\sqrt{c+iu+\lambda^2}} \right|
\end{aligned}
$$

For $|c|$ sufficiently large and any fixed λ the quantity $|\sqrt{c+iu}/\sqrt{c+iu+\lambda^2}|$ is arbitrarily close to 1 (uniformly in u) and we have from above

$$
\begin{aligned}
& Ce^{c(t-T)} \left| \int_{-\infty}^{\infty} \frac{\sqrt{c+iu}\,du}{\sinh(\sqrt{c+iu})\sinh(\sqrt{c+iu+\lambda^2})\sqrt{c+iu+\lambda^2}} \right| \\
\leq\; & Ce^{c(t-T)} \left| \int_{-\infty}^{\infty} \frac{du}{\sinh(\sqrt{c+iu})\sinh(\sqrt{c+iu+\lambda^2})} \right| \\
\leq\; & Ce^{c(t-T)} \left(\int_{-\infty}^{\infty} \frac{du}{|\sinh(\sqrt{c+iu})|^2} \right)^{1/2} \left(\int_{-\infty}^{\infty} \frac{du}{|\sinh(\sqrt{c+iu+\lambda^2})|^2} \right)^{1/2} \qquad (4.28)
\end{aligned}
$$

We now make use of the identity $|\sinh(\sqrt{c+iu})|^2 = \sin^2(p_1) + \sinh^2(p_2)$ where $p_1 = \sqrt{(-c+\sqrt{c^2+u^2})/2}$ and $p_2 = \sqrt{(c+\sqrt{c^2+u^2})/2}$; note that p_1 and p_2 are real. It's easy to see that for $|c| < |u|$ and since $c < 0$ we have $p_2 \geq u/\sqrt{2}$ so that

$$
\begin{aligned}
\int_{|u|>|c|} \frac{du}{|\sinh(\sqrt{c+iu})|^2} &= \int_{|u|>|c|} \frac{du}{\sin^2(p_1) + \sinh^2(p_2)} \\
&\leq \int_{|u|>|c|} \frac{du}{\sinh^2(p_2)}
\end{aligned}
$$

$$
\begin{aligned}
&\leq \int_{|u|>|c|} \frac{du}{\sinh^2(\frac{u}{\sqrt{2}})} \\
&= \frac{4\sqrt{2}}{e^{\sqrt{2}|c|}-1}.
\end{aligned}
$$

If we choose of the form $c = -\pi^2(2k+1/2)^2$ for $k \in \mathbf{Z}$ then $\frac{1}{|\sinh(\sqrt{c+iu})|^2} \leq 1$ for all u, so that $\int_{-|c|}^{|c|} \frac{du}{|\sinh(\sqrt{c+iu})|^2} \leq 2|c|$. Combining this with the above estimates shows that

$$
\int_{-\infty}^{\infty} \frac{du}{|\sinh(\sqrt{c+iu})|^2} \leq \left(\frac{4\sqrt{2}}{e^{\sqrt{2}|c|}-1} + 2|c|\right) \leq \tilde{C}|c|
$$

for some constant $\tilde{C}$ and for $|c|$ sufficiently large. A similar estimate can be made for the second integral on the right in (4.28), noting that if λ is fixed then the choice $c = -\pi^2(2k+1/2)^2$ still avoids the poles in the integrand for sufficiently large k. All in all we find from (4.28) that

$$
\left| \int_{c-i\infty}^{c+i\infty} e^{st} \frac{e^{st}\hat{g}(s)\sqrt{s}\,ds}{\sinh(\sqrt{s})\sinh(\sqrt{s+\lambda^2})\sqrt{s+\lambda^2}} \right| \leq Ce^{c(t-T)}|c|
$$

which, since $t - T > 0$, clearly tends to zero as $c \to -\infty$ as $c = -\pi^2(2k+1/2)^2$.

We can thus compute $K(t,\lambda)$ by computing the residues of $e^{st}M(s,\lambda)\hat{g}(s)$ in the left half plane. The poles occur in the function $M(s,\lambda)$; straightforward calculations (still assuming that $\lambda^2 \neq \pi^2(k^2-j^2)$ for integers j,k) show that $M(s,\lambda)$ has simple poles at $s = -k^2\pi^2$ with residue $r_1(k)$ and at $s = -k^2\pi^2 - \lambda^2$ with residue $r_2(k)$, where $r_1(k)$ and $r_2(k)$ are given by equations (4.25) and (4.26), respectively. It then follows from the residue theorem applied to the integrand in equation (4.27) that $K(t,\lambda)$ is given by the series (4.24).

The above analysis was done under the assumption that $\lambda^2 \neq \pi^2(k^2-j^2)$ for integers j,k; if this is not true then one or more of the simple poles may "coalesce" into a quadratic pole and a slightly different residue computation is needed. However, it is easy to see that the value of $K(t,\lambda)$ must depend continuously on λ, and so we will simply write equation (4.24) with the understanding that in the exceptional cases for λ the correct value is obtained by continuity. ■

One special case that is worth noting, however, is $\lambda = 0$. In this case a residue computation shows that

$$
K(t,0) = \hat{g}(0) + \sum_{k=1}^{\infty} r(k)e^{-k^2\pi^2 t}
$$

HW – 7A – for Friday

Find the Laurent series for $f(z) = 1/(z^2+z)$ in the following regions:

① $0 < |z| < 1$

② $0 < |z-1| < 1$

③ $1 < |z-1| < 2$

Represent the function $f(z) = 1/(z^3 - z)$ in the following regions:

④ $0 < |z| < 1$

⑤ $1 < |z|$

⑥ $0 < |z-1| < 1$

⑦ $1 < |z-1| < 2$

Find the proper infinite series representation for $f(z) = z/(z^2+z-2)$ in the regions:

⑧ $|z| < 1$

⑨ $0 < |z-1| < 3$

⑩ $0 < |z+2| < 3$

⑪ $1 < |z| < 2$

⑫ $|z| > 2$

⑬ $|z+2| > 3$

- singularities
  - non-isolated
  - isolated
    - poles
      - simple
      - of order m ≠
    - removable
    - essential

Examples :

(1) $1 / \sin\left(\frac{\pi}{z}\right)$: $z = 0$ non-isolated

$z = \frac{1}{n}$, $n = \pm 1, \pm 2, \ldots$ isolated

(2) $\frac{5z}{z(z-1)} = \frac{2}{z} - 3 - 3z + \cdots$: $z = 0$ simple pole

(3) $\frac{\sinh z}{z^4} = \frac{1}{z^3} + \frac{1}{6z} + \frac{1}{120} z + \cdots$: $z = 0$

pole of order 3

(4) $\frac{e^z - 1}{z} = 1 + \frac{z}{2} + \frac{z^2}{6} + \cdots$: $z = 0$ removable

(5) $\exp\left(\frac{1}{z}\right) = \sum_{n=0}^{\infty} \frac{1}{n!} \frac{1}{z^n}$: $z = 0$ essential

where $r(k)$ denotes $2\hat{g}(-k^2\pi^2) - 4k^2\pi^2[\hat{g}'(-k^2\pi^2) + t\hat{g}(-k^2\pi^2)]$.

It is also worth noting that we can similarly compute $K(t_0, \lambda)$ for times $t_0 < T$, or under the assumption that $g(t)$ does not have compact support. In this case we split $g(t) = g_1(t) + g_2(t)$ with g_1 supported in $[0, t_0]$ and g_2 supported in $[t_0, \infty)$. The function $K(t_0, \lambda)$ can be computed by doing two contour integrals, one corresponding to g_1, the other to g_2. The contour for g_1 is as before, around the left half plane. The appropriate contour for g_2 is around the right half plane, and in fact evaluates to zero since $M(s, \lambda)$ has no poles there. This is really an expression of causality—what the flux does at times $t > t_0$ has no effect on $K(t_0, \lambda)$ or the data $d(t_0, \lambda)$.

It is instructive to examine the function $K(t, \lambda)$ in the special case that the flux is $g(t) = \delta(t)$, an impulse at time $t = 0$. Figure 2 below shows $K(t, \lambda)$ in two dimensions (so λ is a scalar) as a function of t for several different values of λ.

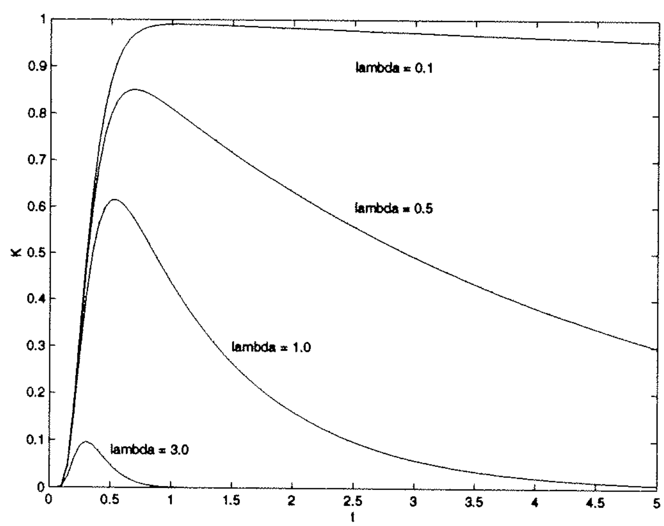

Figure 2: Function $K(t, \lambda)$ for several values of λ.

Note that the peak value of K drops rapidly as λ increases, and that K decreases rapidly in t. This illustrates that there is an optimal time window for making measurements, an issue we will explore below.

4.2 Uniqueness, Stability, and Reconstruction

Equation (4.24) shows that the relation between the Fourier coefficients $\hat{d}(t, \lambda)$ and the Fourier coefficients $\hat{S}(\lambda)$ of the function S is given at any time t as

$$\hat{d}(t, \lambda) = K(t, \lambda)\hat{S}(\lambda). \tag{4.29}$$

We can simply recover the Fourier coefficients of $\hat{S}$ from measurements taken at any given time $t = t_0$ as

$$\hat{S}(\lambda) = \frac{\hat{d}(t_0, \lambda)}{K(t_0, \lambda)},$$

provided of course that $K(t_0, \lambda) \neq 0$. Again, however, as in the Laplace "s" domain, such an estimate magnifies error by a factor proportional to $|\lambda|e^{|\lambda|}$.

In practice, one has data from time $t = t_1$ to time $t = t_2$, and it makes sense to use all of the data in any reconstruction. Realistically, however, the data will be noisy, and hence provide no consistent estimate of $\hat{S}$ or S. In this case we might attempt to estimate $\hat{S}(\lambda)$ by choosing that function which minimizes the error

$$\int_{t_1}^{t_2} [\hat{d}(t, \lambda) - K(t, \lambda)\hat{S}(\lambda)]^2 \, dt.$$

The minimizer is easily found to be

$$\hat{S}(\lambda) = \frac{\int_{t_1}^{t_2} K(t, \lambda)\hat{d}(t, \lambda) \, dt}{\int_{t_1}^{t_2} K^2(t, \lambda) \, dt}. \tag{4.30}$$

This is the scheme we use in our reconstructions, with a few adaptive modifications discussed below.

The series formula (4.24) converges rapidly for $t > T$, sufficiently rapidly that $K(t, \lambda)$ is analytic in t for $t > T$. It follows that $K(t, \lambda)$ cannot vanish on any open interval $t_1 < t < t_2$, and so (in the absence of noise) the estimate (4.30) will recover $\hat{S}$, and so S. This is a stronger version of uniqueness than previously stated:

Lemma 4.2 *For the linearized inverse problem with flux $g = g(t)$ and constant initial condition, the data $d(t, x')$ over any interval $t_1 < t < t_2$ uniquely determines $S(x')$.*

From equation (4.30) on can also obtain a stability estimate for the estimate of $\hat{S}(\lambda)$. For simplicity, let us consider the case $t_1 = 0$, $t_2 = \infty$. Let the actual back surface be $S_0(x')$ with

Fourier cosine coefficients $\hat{S}_0(\lambda)$, and "true" data (for the linearized problem) $d_0(t,x')$ with Fourier expansion $\hat{d}_0(t,\lambda)$. Let the actual noisy data be given by $d(t,x') = d_0(t,x') + e(t,x')$, with Fourier coefficients $\hat{d}_0(t,\lambda) + \hat{e}(t,\lambda)$. The estimate based on (4.30) produces

$$\hat{S}(\lambda) = \hat{S}_0(\lambda) + \frac{\int_0^\infty K(t,\lambda)\hat{e}(t,\lambda)\,dt}{\int_0^\infty K^2(t,\lambda)\,dt}.$$

Let $\hat{E}(\lambda) = \hat{S}(\lambda) - \hat{S}_0(\lambda)$. An elementary estimate with Parseval's inequality yields

$$|\hat{E}(\lambda)|^2 \leq \frac{\int_0^\infty \hat{e}^2(t,\lambda)\,dt}{\int_0^\infty K^2(t,\lambda)\,dt}, \tag{4.31}$$

provided that the numerator is finite. We can bound the denominator away from zero in terms of λ by first noting that, by Plancherel's Theorem,

$$\int_0^\infty K^2(t,\lambda)\,dt = \int_{-i\infty}^{i\infty} |M(s,\lambda)|^2\,ds \tag{4.32}$$

with M given by (4.23). Parameterize the integral as $s = iu$ with u real. A bit of tedious algebra shows that

$$|K(iu,\lambda)|^2 = \frac{u|\hat{g}(iu)|^2}{\sqrt{\lambda^4+u^2}\left(\cosh^2(p_2) - \cos^2(p_1)\right)\left(\cosh^2(\sqrt{u/2}) - \cos^2(\sqrt{u/2})\right)} \tag{4.33}$$

where $p_1 = \sqrt{(\sqrt{\lambda^4+u^2} - \lambda^2)/2}$ and $p_2 = \sqrt{(\sqrt{\lambda^4+u^2} + \lambda^2)/2}$. From (4.33) one can rather easily obtain a bound of the form

$$\int_0^\infty |M(iu,\lambda)|^2\,du \geq \frac{C}{\lambda^2 e^{2\lambda}}$$

for some constant C. Combining this with equations (4.31) and (4.32) we then have

Lemma 4.3 *Let the estimate of $\hat{S}$ be constructed according to equation (4.30) on the interval $0 < t < \infty$. Then the error in the estimate $\hat{S}(\lambda)$ is bounded as*

$$|\hat{S}(\lambda) - \hat{S}_0(\lambda)| \leq C|\lambda|e^{|\lambda|}\left(\int_0^\infty \hat{e}^2(t,\lambda)\,dt\right)^{1/2}.$$

It is fairly easy to construct examples showing that this is the best possible continuous dependence result.

Remark 4.1 *We obtained equations (2.2)-(2.5) by rescaling the original equations (2.1) and the associated boundary and initial condition. If we account for the effect of the sample* *depth d find that λ should be replaced by $d\lambda$, and the continuous dependence result Lemma 4.3 yields*

$$|\hat{S}(\lambda) - \hat{S}_0(\lambda)| \leq C|d\lambda|e^{|d\lambda|}\left(\int_0^\infty \hat{e}^2(t,\lambda)\,dt\right)^{1/2}. \tag{4.34}$$

Thus the ability to resolve high frequency detail drops off exponentially with sample depth.

Also, by considering the rescaling in time we see that the characteristic time scale for the problem is $\frac{d^2}{\alpha}$. As a result larger diffusivities compress the period in which measurements should be taken. That the time scale is proportional to the square of the sample depth has been noted elsewhere.

4.3 Examples

Below we present several reconstruction examples. In all but the last two figures the "uncorroded" or reference sample region Ω_0 was taken as the two dimensional region $(0, 10) \times (0, 1)$ in the xy plane. The region Ω whose back surface is to be recovered is given by $\{(x, y); 0 < x < 10, S(x) < y < 1\}$, where S is a C^1 function with compact support in $(0, 10)$. Data for the heat equation on Ω was generated by first transforming the heat equation and associated conditions (2.2)-(2.5) to the modified equation and boundary conditions (2.6)-(2.9) (but NOT linearizing). We then solve (2.6)-(2.9) on Ω_0 using a Crank-Nicholson differencing scheme. Typical grid sizes were 50 to 100 nodes in the x direction, 30 to 40 in the y direction, with 20 to 60 time steps. The large linear systems at each time step were solved with a preconditioned conjugate gradient method.

The reconstruction was done in Matlab with a straightforward implementation of equation (4.30). First note that the data appearing in (4.30) is the *perturbation* in the temperature response caused by corrosion. We thus first compute the temperature response of the reference region Ω_0 and subtract this from the data generated for Ω. We then compute the finite cosine transform of the data at each time step using an FFT-based algorithm; the function $K(t, \lambda)$ is implemented with equation (4.24), truncated after 30 terms. The integral in equation (4.30) is computed simply with the trapezoidal rule. The reconstructions are extremely fast—on the order of one second with 64 data points on the top surface times 40 time samples.

There is one other modification we make to the implementation. If one considers Figure 2, it is apparent that for certain frequency-time combinations the value of $K(t, \lambda)$ is so small that the corresponding Fourier cosine frequencies should not be used. We thus perform a thresholding—if $|K(t, \lambda)| < \epsilon$ for some chosen value (which should depend on the noise level in the data), then the corresponding points are automatically omitted from the reconstruction based on equation (4.30). This turns out to be an enormous improvement over a straight implementation of equation (4.30), especially for large λ, for in examination of Figure 2 it is apparent that for higher frequencies one has a rather small "window of opportunity" for capturing the relevant information in the signal. Nonetheless, if λ is sufficiently large, it may turn out that no stable estimate of $\hat{S}(\lambda)$ is possible (as in our last example).

In the first example we use the back surface defined by $S(x) = 0.1f(2.5, 7.5, x)$ where

$$f(a, b, x) = \frac{64}{(b-a)^6}(x-a)^3(b-x)^3 \tag{4.35}$$

(see Figure 3). The input flux was $g(t) = 10$ for $0 < t < 0.1$, 0 for $t > 0.1$, and zero initial conditions were used. Data was taken a 64 equally spaced points on the top surface for 40 equally spaced time intervals from $t = 0.1$ to $t = 4.0$ (examination of $K(t, \lambda)$ shows that this is the time interval in which most of the information should lie). The solid line in Figure 3 represents the actual back surface, the dashed line is the reconstruction. For this figure a threshold of 0.01 was used, i.e., those values of $K(t, \lambda) < 0.01$ and the corresponding data were discarded, although even at the highest frequency at least one value of K remained for at least one time slice. The data was noiseless, down to the resolution of the heat equation solver (about 4 significant figures). Note that the estimate slightly overshoots. This is typical, and due to the fact that the linearized model of the material loss for the forward problem predicts smaller temperature perturbations than the full nonlinear model. As a result, an inverse solver based on the linear model must "overestimate" the back surface corrosion in order to obtain the same temperature perturbation.

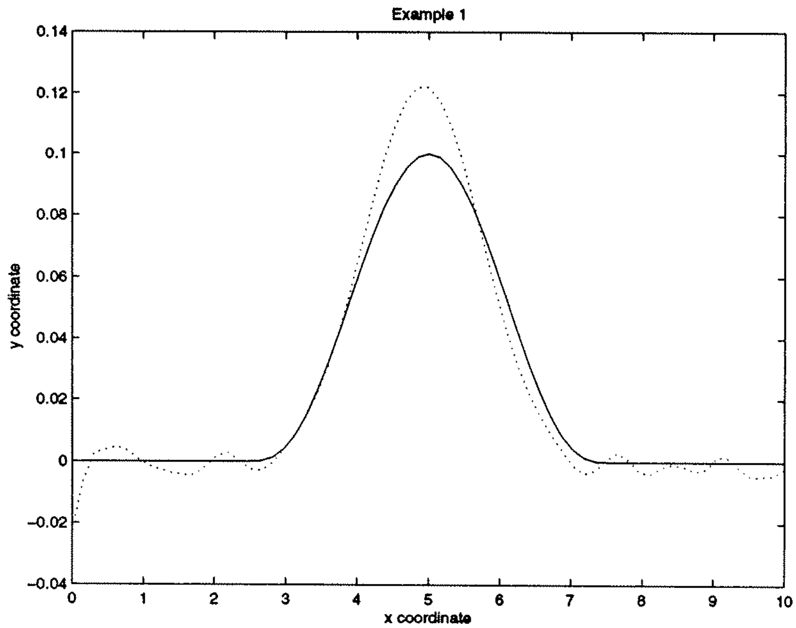

Figure 3

Let us consider another more challenging example, in which the back surface is defined by $S(x) = 0.1f(4,6,x) + 0.08f(5,8,x)$, with f given by (4.35). With noiseless data and the same parameters as example 1 we obtain the reconstruction shown in Figure 4.

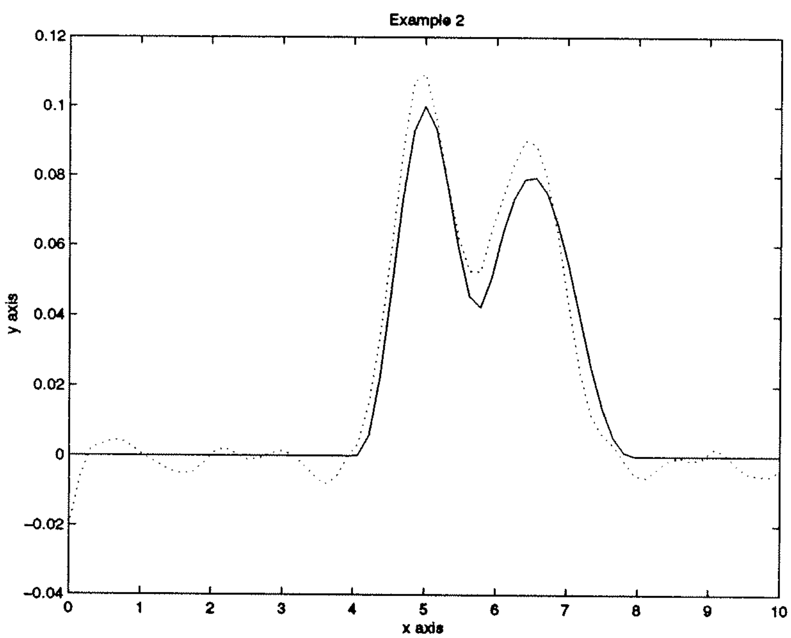

Figure 4

However, if we add noise to the data in the previous example the reconstruction becomes considerably more difficult. For the following example we add Gaussian noise to the data from Figure 4, independent in both the x and t variables, with zero mean and variance equal to 10 percent of the RMS strength of the *perturbed* signal $u - u_0$. The result, with regularization $\epsilon = 0.01$, is the rather unsatisfactory estimate below:

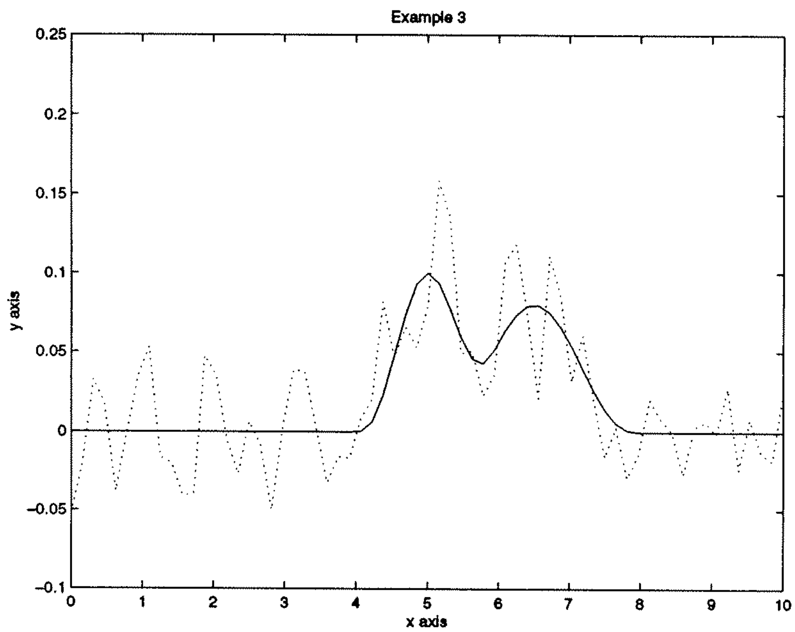

Figure 5

Increasing the regularization to $\epsilon = 0.1$ results in the reconstruction shown in Figure 6. Although the estimate has been smoothed, the ability to distinguish the peaks is lost.

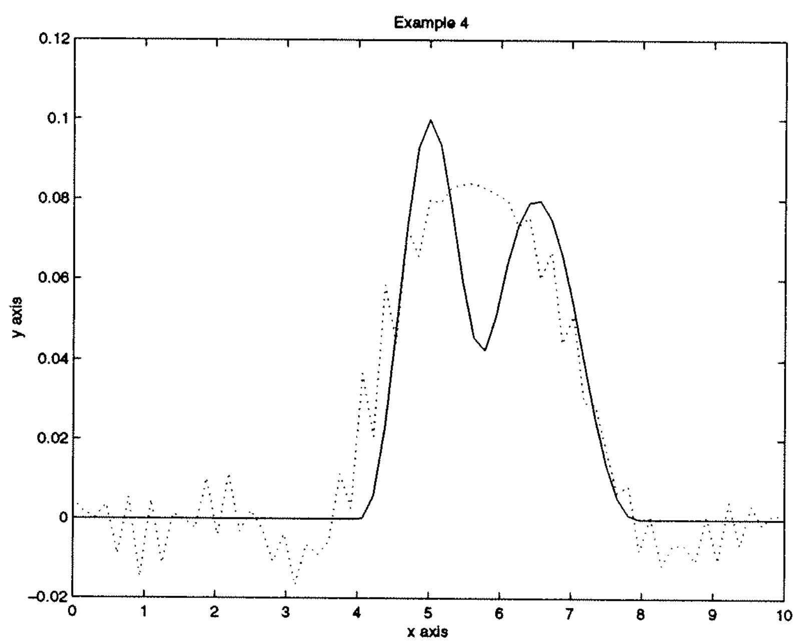

Figure 6

We now present an example to illustrate the difficulty of increasing sample depth in estimating the back surface profile. In Figure 7 we consider a simulated sample made of aluminum (thermal diffusivity $\alpha = 0.946\frac{\text{cm}^2}{\text{sec}}$), sample thickness 0.5 cm, with the sample length 5.0 cm. The back surface profile is given by $S(x) = 0.05f(2, 3, x) + 0.04f(2.5, 4, x)$, about 10 percent of the plate thickness. We use an input flux $g(t) = 1$ for $0 < t < 0.1$ seconds, and 0 for $t > 0.1$ seconds. Examination of the rescaled variable $\tilde{t} = \frac{\alpha}{d^2}t \approx 3.785t$ and Figure 2 shows that the first second of data should contain the all of the relevant information concerning S. We thus take data from time $t = 0.1$ to $t = 1.1$ seconds. The data contains 10 percent RMS noise, and the recovered estimate with $\epsilon = 0.01$ is as shown in Figure 7.

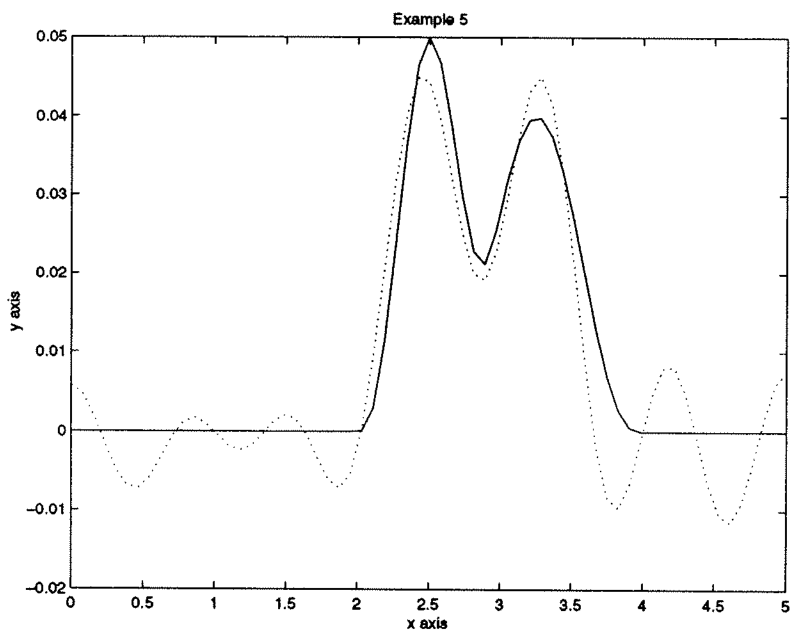

Figure 7

If the sample depth is increased to 1.0 cm and the other parameters kept the same (including the noise level, kept at 10 percent of the signal strength for the *data used in Figure 7*), the estimate with $\epsilon = 0.01$ is as shown in Figure 8. Decreasing ϵ to 0.001 results in little change in the estimate, but any further decrease results in a hopelessly noisy reconstruction. Increasing ϵ to 0.1 results in a reconstruction that is identically zero.

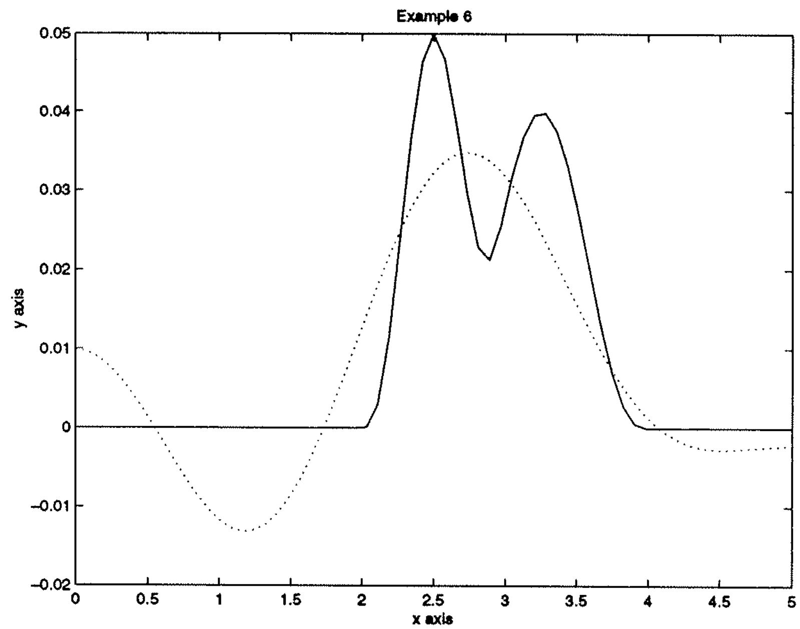

Figure 8

If we increase the sample depth to 1.5 cm we find that (with this noise level) no satisfactory estimate of the back surface can be obtained. This illustrates the fact quantified in equation (4.34)—resolution and stability of the estimates decay exponentially with increasing sample depth.

5 Conclusion

Our analysis in this paper shows that by linearizing and using appropriate test functions one can extract relevant information concerning the back surface profile of a sample from front surface temperature measurements in thermal imaging. With such an approach one can prove uniqueness and continuous dependence results for the inverse problem, as well as recover back surface estimates and regularize the inversion in an insightful way.

The approach here should extend in some form to a broader setting. The idea of linearizing with respect to the unknown portion of the boundary of the sample extends to more general domains (we have already worked out the details in a fairly general setting). In this case one can also use suitable test functions to extract information about the unknown part of the surface from temperature measurements, although the test functions cannot typically be written down explicitly as we have done here. Nonetheless, one might construct such test functions numerically and use a similar approach to reconstruction.

In the present and more general setting it would also be interesting to consider what type of input flux is optimal, in the sense of giving maximum resolution and/or stability for a given input energy. It should be possible to construct such a flux, probably numerically, by some variation of the "power method" for finding the largest eigenvalue for a linear operator. Such an approach has been used to find optimal input fluxes for the impedance imaging problem [10].

And although we considered a reconstruction scheme only for the case in which the flux is spatially constant, it would be interesting to see whether the technique used in the third case case of the uniqueness theorem—finding a first order PDE satisfied by $S(x')$—could be used as the basis of a reconstruction algorithm.

6 Bibliography

References

[1] Banks, H.T., F. Kojima and W.P. Winfree, *Boundary estimation problems arising in thermal tomography,* Inverse Problems 6 (1990), pp. 897-922.

[2] K. Bryan and L.F. Caudill, Jr., *An inverse problem in thermal imaging*, SIAM J. Appl. Math., 56 (1996), pp. 715–735.

[3] K. Bryan and L.F. Caudill, Jr., *A uniqueness theorem for an inverse problem in thermal imaging*, presented at the third Mississippi State Conference on Differential Equations and Computational Simulations (1997), and to appear in the Electronic Journal of Differential Equations.

[4] K. Bryan, *A boundary integral method for an inverse problem in thermal imaging.*, Journal of Systems, Estimation, and Control, 7, (1997), pp. 1-27.

[5] D. J. Crowther, L. D. Favro, P. K. Kuo, and R. L. Thomas, *An inverse scattering algorithm applied to infrared thermal wave images*, J. Appl. Phys. 74, (1993) pp. 5828-5834.

[6] L. D. Favro, D. J. Crowther, P. K. Kuo, and R. L. Thomas, *Inverse scattering of pulsed thermal waves*, in Advances in Signal Processing for Nondestructive Evaluation of Materials, X.P.V. Maldague, Ed., Kluwer Academic Publishers, the Netherlands, (1994) pp. 187-191.

[7] L. D. Favro, T. Ahmed, X. Han, L. Wang, X. Wang, P. K. Kuo, and R. L. Thomas, *Thermal wave imaging of disbonding and corrosion on aircraft*, Review of Progress in Quantitative NDE, Vol. 15, edited by D. O. Thompson and D. Chimenti, Plenum, New York, (1996).

[8] R. Courant and D. Hilbert, *Methods of Mathematical Physics*, Wiley, New York, 1989.

[9] D. Gilbarg and N. Trudinger, *Elliptic Partial Differential Equations of Second Order* (Second Edition), Springer-Verlag, Berlin, 1983.

[10] Gisser, D.G., D. Isaacson, and J.C. Newell, *Electric current computed tomography and eigenvalues*, SIAM J. Appl. Math, 50(6) (1990), pp. 1623-1634.

[11] O. Ladyzhenskaya, V. Solonnikov, and N. Uraltseva, *Linear and Quasilinear Equations of Parabolic Type* (Translations of Mathematical Monographs, v. 23), American Mathematical Society, Providence, RI, 1968.

[12] L. Nirenberg, *Uniqueness in Cauchy problems for differential equations with constant leading coefficients*, Comm. Pure Appl. Math. 10 (1957), pp. 89-105.

[13] J.C. Saut and B. Scheurer, *Unique continuation for some evolution equations*, J. Differential Equations 66 (1987), 118-139.

7 Appendix: An Integral Identity

In this section we derive the identity (3.14).

Let Ω_T denote $\Omega \times [0,T]$, $\partial\Omega_T$ denote $\partial\Omega \times [0,T]$, P_1 denote $(x_n = 1) \times [0,T]$ and P_0 denote $\partial\Omega_T \setminus P_1$ for some fixed time $T > 0$. Let $\phi(x,t)$ be a sufficiently smooth test function defined on Ω_T with $\phi_t + \Delta\phi = 0$ and $\phi(T,x) \equiv 0$ for $x \in \Omega$. Also, let us take $\frac{\partial\phi}{\partial\nu} = 0$ on $\partial\Omega \setminus P_1$. Throughout we treat $S(x')$ as a function of all n spatial variables, which just happens not to depend on x_n, so $\frac{\partial S}{\partial x_n} = 0$.

Multiply the left side of the linearized heat equation (2.10) by ϕ and integrate the first term by parts in t and the second by parts in x to obtain

$$\int_{\Omega_T} \left(\phi \frac{\partial u}{\partial t} - \phi \,\Delta\, u \right) dx\, dt = \int_{\partial\Omega_T} \left(u \frac{\partial\phi}{\partial\nu} - \phi \frac{\partial u}{\partial\nu} \right) dx'\, dt - \int_\Omega u\phi|_{t=0}\, dx.$$

where we have used $\frac{\partial\phi}{\partial t} + \Delta\phi = 0$. From the boundary conditions (2.11) and (2.12) for the linearized problem the right side above yields

$$\begin{aligned}\int_{\Omega_T} \left(\phi \frac{\partial u}{\partial t} - \phi \,\Delta\, u \right) dx\, dt &= \int_{P_1} u \frac{\partial\phi}{\partial\nu}\, dx'\, dt + \int_{P_1} S\phi g\, dx'\, dt \\ &+ \int_{P_0} \phi\nabla S \cdot \nabla u_0\, dx'\, dt - \int_\Omega u\phi|_{t=0}\, dx. \end{aligned} \qquad (7.36)$$

Now we turn to the right side of the linearized heat equation (2.10). Multiply the right side of equation (2.10) by ϕ and use the identity

$$\phi\nabla\cdot(\kappa\nabla u_0) = \nabla\cdot(\phi\kappa\nabla u_0) - (\nabla\phi)\cdot\kappa\nabla u_0$$

and the divergence theorem to obtain (using $n\cdot(\phi S\nabla u_0) = S\phi g$ on P_1, 0 on P_0, and $n\cdot(\phi\kappa\nabla u_0) = S\phi g$ on P_1, $\phi\nabla S\cdot\nabla u_0$ on P_0)

$$\begin{aligned}\int_{\Omega_T} \phi\,(\nabla\cdot\kappa\nabla u_0 + S\,\Delta\, u_0)\, dx\, dt &= \int_{P_0} \phi\nabla S\cdot\nabla u_0\, dx'\, dt - \int_{\Omega_T} \nabla\phi\cdot\kappa\nabla u_0\, dx\, dt \\ &+ 2\int_{P_1} S\phi g\, dx'\, dt - \int_{\Omega_T} \nabla(\phi S)\cdot\nabla u_0\, dx\, dt. \end{aligned} \qquad (7.37)$$

Using equation (2.10) to equate the right sides of equations (7.36) and (7.37), and using the initial conditions, we find that

$$\int_{P_1} u\frac{\partial\phi}{\partial\nu}\, dx'\, dt = \int_\Omega (1-x_n) S\phi \frac{\partial u_0}{\partial x_n}|_{t=0}\, dx + \int_{P_1} S\phi g\, dx'\, dt - \int_{\Omega_T} (\nabla\phi\cdot\kappa\nabla u_0 + \nabla(\phi S)\cdot\nabla u_0)\, dx\, dt. \qquad (7.38)$$

If we expand the integral over Ω_T in equation (7.38) out in terms of u_0, ϕ, and S we obtain

$$-\int_{\Omega_T}(\nabla\phi\cdot\kappa\nabla u_0+\nabla(\phi S)\cdot\nabla u_0)\,dx\,dt$$
$$=\int_{\Omega_T}\left[(1-x_n)\left(\frac{\partial u_0}{\partial x_n}\nabla S\cdot\nabla\phi+\frac{\partial\phi}{\partial x_n}\nabla S\cdot\nabla u_0\right)-2S\frac{\partial u_0}{\partial x_n}\frac{\partial\phi}{\partial x_n}-\phi\nabla u_0\cdot\nabla S\right]\,dx\,dt \quad (7.39)$$

Now let us apply the identity $a\nabla b\cdot\nabla c=\nabla\cdot(ac\nabla b)-ac\,\triangle\, b-c\nabla a\cdot\nabla b$ to the terms on the right above which involve ∇S. With S playing the role of c we obtain (using the various boundary conditions on ϕ, u_0, and the divergence theorem)

$$\begin{aligned}-\int_{\Omega_T}(\nabla\phi\cdot\kappa\nabla u_0 &+ \nabla(\phi S)\cdot\nabla u_0)\,dx\,dt=-\int_{P_1}S\phi g\,dx'\,dt+\int_{\Omega_T}S\nabla\phi\cdot\nabla u_0\,dx\,dt\\ &-\int_{\Omega_T}\left[(1-x_n)S\left(\frac{\partial\phi}{\partial x_n}\triangle u_0+\frac{\partial u_0}{\partial x_n}\triangle\phi\right)-S\phi\triangle u_0\right]\,dx\,dt\\ &-\int_{\Omega_T}S(1-x_n)\frac{\partial}{\partial x_n}(\nabla u_0\cdot\nabla\phi)\,dx\,dt.\end{aligned}$$

Replace $\triangle\phi=-\frac{\partial\phi}{\partial t}$ and $\triangle u_0=\frac{\partial u_0}{\partial t}$ and integrate the last term on the right above by parts in x_n to obtain some nice cancellations and

$$-\int_{\Omega_T}(\nabla\phi\cdot\kappa\nabla u_0+\nabla(\phi S)\cdot\nabla u_0)\,dx\,dt=-\int_{P_1}S\phi g\,dx'\,dt$$
$$-\int_{\Omega_T}\left[(1-x_n)S\left(\frac{\partial\phi}{\partial x_n}\frac{\partial u_0}{\partial t}-\frac{\partial u_0}{\partial x_n}\frac{\partial\phi}{\partial t}\right)-S\phi\triangle u_0\right]\,dx\,dt+\int_{P_0}S\nabla\phi\cdot\nabla u_0\,dx'\,dt \quad (7.40)$$

Integrate the second term under the Ω_T integral by parts in t

$$-\int_{\Omega_T}(\nabla\phi\cdot\kappa\nabla u_0+\nabla(\phi S)\cdot\nabla u_0)\,dx\,dt=-\int_{P_1}S\phi g\,dx'\,dt$$
$$-\int_{\Omega_T}\left[(1-x_n)S\left(\frac{\partial\phi}{\partial x_n}\frac{\partial u_0}{\partial t}+\frac{\partial^2 u_0}{\partial x_n\partial t}\phi\right)-S\phi\triangle u_0\right]\,dx\,dt+\int_{P_0}S\nabla\phi\cdot\nabla u_0\,dx'\,dt$$
$$-\int_{\Omega}(1-x_n)S\phi\frac{\partial u_0}{\partial x_n}|_{t=0}\,dx. \quad (7.41)$$

Finally, integrate the mixed partial term by parts in x_n; all terms in the Ω_T integral cancel and we obtain

$$-\int_{\Omega_T}(\nabla\phi\cdot\kappa\nabla u_0+\nabla(\phi S)\cdot\nabla u_0)\,dx\,dt=-\int_{P_1}S\phi g\,dx'\,dt$$
$$+\int_{P_0}(S\nabla\phi\cdot\nabla u_0+S\phi\triangle u_0)\,dx'\,dt-\int_{\Omega}(1-x_n)S\phi\frac{\partial u_0}{\partial x_n}|_{t=0}\,dx. \quad (7.42)$$

Now use equation (7.42) to replace the corresponding term on the right in equation (7.38). We obtain

$$\int_{P_1} u \frac{\partial \phi}{\partial \nu} \, dx' \, dt = \int_{P_0} (S \nabla \phi \cdot \nabla u_0 + S \phi \triangle u_0) \, dx' \, dt$$

or

$$\int_{P_1} u \frac{\partial \phi}{\partial \nu} \, dx' \, dt = \int_{P_0} (\nabla \cdot \phi \nabla u_0) S \, dx' \, dt. \tag{7.43}$$

This equation expresses the boundary data (or really, a weighted integral of the boundary data) in terms of integrals involving the function S. Note that u_0 and ϕ are known functions.

One minor modification can be made. Let us take ϕ to satisfy the *forward* heat equation with $\frac{\partial \phi}{\partial \nu} \equiv 0$ on R_0 and $\phi(0, x) \equiv 0$. Modify the linearized inverse problem appropriately (noting that $\phi(T-t, x)$ satisfies the backward heat equation with the appropriate conditions). Equation (7.43) becomes exactly equation (3.14) in the text.